4080 *Chem. Mater.* **2009,** *21,* 4080–4086
DOI:10.1021/cm902015f

CHEMISTRY OF MATERIALS
Article

Nanocasting of High Surface Area Mesoporous Ga_2O_3 and GaN Semiconductor Materials

Colin West and Robert Mokaya*

School of Chemistry, University of Nottingham, University Park, Nottingham NG7 2RD, United Kingdom

Received July 6, 2009

We report mesostructured gallium oxide and nanoporous gallium nitride, synthesized via a nanocasting technique using mesoporous carbon as template. The carbon template is first loaded with a gallium chloride toluene solution to generate a Ga precursor/carbon composite. Gallium oxide is generated by reaction of the composite in air during calcination, which also eliminates the carbon template. Formation of mesostructured Ga_2O_3 requires a two-stage oxidation reaction, first at 450 °C and followed by 500 °C. X-ray diffraction, nitrogen physisorption, and transmission electron microscopy show the Ga_2O_3 products to be mesostructured with a very high surface area of 307 m^2/g and pore volume of 0.54 cm^3/g. The Ga_2O_3 exhibits a band gap energy of 4.6 eV. Thermal treatment of the Ga/carbon composite in the presence of ammonia (i.e., nitridation) generates crystalline nanoporous GaN with surface area of 136−156 m^2/g and pore volume of 0.3−0.4 cm^3/g.

1. Introduction

Highly porous metal oxide materials have a wide range of potential applications including molecular separation, sorption, drug delivery, or use as catalysts and catalyst supports.[1,2] Materials with long-range ordering of the pore channel network and uniform pore sizes open up an even wider range of potential applications.[2] The early synthesis of ordered mesoporous silica materials utilized self-assembled surfactant micelles as templates for inorganic silica precursors.[3] Surfactant templating of mesoporous materials has since been extended to produce a number of highly ordered silica materials with a variety of cubic/hexagonal mesophases, two or three-dimensional interconnected pore networks and various tunable properties including pore size, pore size distribution and wall thickness.[4] Extending this surfactant based 'soft templating' process to produce non-siliceous mesoporous materials has been of great interest, particularly for ordered mesoporous metal oxides and nitrides. Some successful methods have been developed[5] though there still remains no general route for synthesizing some desirable metal oxides and nitrides that so far remain inaccessible via soft templating methods. One major drawback is that without precise control during the oxidation or nitridation process, the growth of many metal oxide and nitride crystal structures (which crystallize more readily than silica) may become undirected and uncontrolled, causing the breakdown of any ordered mesostructure. Additionally the redox stability of some metal oxides and nitrides can lead to destructive redox reactions with the soft (usually surfactant) template during the calcination step.

An alternative route is to nanocast porous metal oxides/nitrides via sacrificial solid templating whereby an ordered framework (formed from suitable inorganic molecular precursors) of the desired material is fabricated within the pore channels of a porous solid template, followed by the selective removal of the template.[6−12]

*Corresponding author. E-mail: r.mokaya@nottingham.ac.uk.

(1) Davis, M. E. *Nature* **2002**, *417*, 813.
(2) Valdes-Solís, T.; Fuertes, A. B. *Mater. Res. Bull.* **2006**, *41*, 2187.
(3) (a) Kresge, C. T.; Leonowicz, M. E.; Roth, W. J.; Vartuli, J. C.; Beck, J. S. *Nature* **1992**, *359*, 710. (b) Beck, J. S.; Vartuli, J. C.; Roth, W. J.; Leonowicz, M. E.; Kresge, C. T.; Schmitt, K. D.; Chu, C. T.-W.; Olson, D. H.; Sheppard, E. W.; McCullen, S. B.; Higgins, J. B.; Schlenker, J. L. *J. Am. Chem. Soc.* **1992**, *114*, 10834. (c) Yanagisawa, T.; Shimizu, T.; Kuroda, K.; Kato, C. *Bull. Chem. Soc. Jpn.* **1990**, *63*, 988.
(4) (a) Ying, J. Y.; Mehnert, C. P.; Wong, M. S. *Angew. Chem., Int. Ed.* **1999**, *38*, 56. (b) Oye, G.; Sjöblom, J.; Stöcker, M. *Adv. Colloid Interface Sci.* **2001**, *89*, 439. (c) On, D. T.; Desplantier-Giscard, D.; Danumah, C.; Kaliaguine, S. *Appl. Catal. A* **2002**, *222*, 299. (d) Taguchi, A.; Schüth, F. *Microporous Mesoporous Mater.* **2005**, *77*, 1.
(5) (a) Yang, P.; Zhao, D. Y.; Margolese, D. I.; Chmelka, B. F.; Stucky, G. D. *Nature* **1998**, *396*, 152. (b) Schuth, F. *Chem. Mater.* **2001**, *13*, 3184. (c) Soler-Illia, G. J. A. A.; Crepaldi, E. L.; Grosso, D.; Sanchez, C. *Curr. Opin. Colloid Interface Sci.* **2003**, *8*, 109.
(6) Wakayama, H.; Itahara, H.; Tatsuda, N.; Inagaki, S.; Fukushima, Y. *Chem. Mater.* **2001**, *13*, 2392.
(7) (a) Schwickardi, M.; Johann, T.; Schmidt, W.; Schuth, F. *Chem. Mater.* **2002**, *14*, 3913. (b) Lu, A. H.; Schmidt, W.; Taguchi, W.; Spliethoff, A.; Tesche, B.; Schuth, F. *Angew. Chem., Int. Ed.* **2002**, *41*, 3489. (c) Schuth, F. *Angew. Chem., Int. Ed.* **2003**, *21*, 3604. (d) Li, W. C.; Lu, A. H.; Weidenthaler, C.; Schuth, F. *Chem. Mater.* **2004**, *16*, 5676. (e) Lu, A. H.; Schuth, F. *Adv. Mater.* **2006**, *18*, 1793. (f) Waitz, T.; Wagner, T.; Sauerwald, T.; Kohl, C.-D.; Tiemann, M. *Adv. Funct. Mater.* **2009**, *19*, 653. (g) Tiemann, M. *Chem. Mater.* **2008**, *20*, 961. (h) Roggenbuck, J.; Koch, G.; Tiemann, M. *Chem. Mater.* **2006**, *18*, 4151.
(8) Dong, A.; Ren, N.; Tang, Y.; Wang, Y.; Zhang, Y.; Hua, W.; Gao, Z. *J. Am. Chem. Soc.* **2003**, *125*, 4976.
(9) (a) Kang, M.; Yi, S. H.; Lee, H. I.; Yie, J. E.; Kim, J. M. *Chem. Commun.* **2002**, 1944. (b) Kang, M.; Kim, D.; Yi, S. H.; Han, J. U.; Yie, J. E.; Kim, J. M. *Catal. Today* **2004**, *93−95*, 695.
(10) (a) Yang, Z.; Xia, Y.; Mokaya, R. *Adv. Mater.* **2004**, *16*, 727. (b) Xia, Y.; Mokaya, R. *J. Mater. Chem.* **2005**, *15*, 3126. (c) Rushton, B.; Mokaya, R. *J. Mater. Chem.* **2008**, *18*, 235.
(11) (a) Zhu, K.; Yue, B.; Zhou, W. Z.; He, H. Y. *Chem Commun.* **2003**, 98. (b) Shi, Y.; Wan, Y.; Zhang, R. Y.; Zhao, D. Y. *Adv. Funct. Mater.* **2008**, *18*, 2436.
(12) (a) Lee, J.; Han, S.; Hyeon, T. *J. Mater. Chem.* **2004**, *14*, 478. (b) Lee, J.; Kim, J.; Hyeon, T. *Adv. Mater.* **2006**, *18*, 2073.

Published on Web 08/07/2009

Well ordered mesoporous silica materials have been utilized as hard templates in the synthesis of ordered mesoporous carbons[12] and of metal oxides.[11] Ordered mesoporous carbons can also be used as hard templates whereby they may allow replication of the nanocast product back to a structure similar to the original silica template mesostructure.[7,10,13] The advantage of using carbon as template is that it can be easily removed during calcination and in many cases the surface properties of carbon are more amenable to precursor impregnation than silica.[9,14] Although nanocasting requires the additional step of generating the 'hard template' and impregnation with precursor, it offers the advantage of circumventing the difficulties of controlling the assembly of precursor-surfactant systems.[13]

The difficulty of preparing mesoporous semiconductor Ga_2O_3 and GaN materials has long been recognized.[13] Indeed, to date mesoporous Ga_2O_3 stands out as one of the interesting and desirable metal oxides that have not yet been synthesized via either soft sol−gel templating or hard template replication. Ga_2O_3 and GaN exhibit high thermal stability and wide-band gap semiconductivity (with band gap energy of 4.9 and 3.4 eV, respectively) and therefore are potentially useful in optoelectronic devices and high-temperature/high-power electronic devices. Furthermore, Ga_2O_3 has proven potential as a catalyst having been shown to be highly photoactive for mineralizing benzene and its derivatives to CO_2,[15] and is a known water-splitting photocatalyst for the generation of hydrogen gas.[16] Preparation of high porosity Ga_2O_3 and GaN is expected to enhance their use in these surface area dependent applications. Attempts to prepare mesoporous Ga_2O_3 via soft templating have so far been unsuccessful only yielding low surface area and poorly ordered materials. Arean and co-workers prepared disordered mesoporous γ-Ga_2O_3 with surface area of 120 m^2/g,[17] which on calcination at higher temperature yielded β-Ga_2O_3 with a reduced surface area of 40 m^2/g.[18] The preparation of high surface area GaN has also proved difficult, and so far only disordered or nanoparticle forms have been reported.[19] For example, Kam and co-workers prepared porous GaN with surface area of only 50 − 66 m^2/g via the nitridation of γ-Ga_2O_3.[19a] Herein, we describe the synthesis of high surface area Ga_2O_3 and GaN using mesoporous carbon as template. Gallium chloride toluene solution is used as precursor to generate a carbon/$GaCl_3$ composite from which mesoporous Ga_2O_3 is obtained by staged reaction in air. Furthermore, crystalline nanostructured GaN may be obtained via nitridation of carbon/$GaCl_3$ composites. The semiconductor materials synthesized exhibit high surface area and enhanced levels of mesostructural ordering not previously achieved.

2. Experimental Section

2.1. Materials Synthesis. Mesoporous carbon was nanocasted using mesoporous silica SBA-15 via established procedures.[20,21] In brief, for the preparation of SBA-15, a triblock copolymer (Pluronic P123, $EO_{20}PO_{70}EO_{20}$, Aldrich) was used as the structure-directing agent and tetraethylorthosilicate (TEOS) as the silica source.[20] The calcined SBA-15 samples were then used as templates for the preparation of mesoporous carbon as follows: 2 g of SBA-15 was added to a solution of 2.5 g of sucrose, 0.28 g of H_2SO_4, and 10 g of water. This mixture was heated for 6 h at 100 °C and a further 6 h at 160 °C. The solid product was ground and added to a solution of 1.6 g of sucrose, 0.18 g of H_2SO_4, and 10 g of water. The sample was then heated for 6 h at 100 °C and 6 h at 160 °C, followed by carbonization (heating at 20 °C/min to 900 °C then held for 1 h under a flow of nitrogen). After cooling to room temperature, the resulting composite was washed with a 25% HF acid under stirring for 24 h, washed with deionized water and dried at 120 °C to yield mesoporous carbon. To synthesize Ga materials, 0.2 g of mesoporous carbon was added to 0.5 g of $GaCl_3$ in a flask within a nitrogen filled glovebox and the flask sealed. 5.68 mL of sodium dried toluene was added by syringe to the flask to form a 0.5 M solution of $GaCl_3$, and aged under stirring for up to 14 days. A nitrogen-filled balloon was used to preserve an overpressure of nitrogen within the reaction flask. (All equipment including flasks, stoppers, magnetic stirring bars, weighing boats, balloons, syringes, etc., were oven-dried at 100 °C and kept within the glovebox. Syringes were oven-dried immediately prior to use in transferring toluene. Dried balloons were flushed with nitrogen 5 times before use.) The resulting carbon/$GaCl_3$ composite (designated as CMK-3/Ga) was removed from its protective atmosphere, washed with dry toluene and dried under flowing nitrogen at 150 °C. The composite was calcined in a flow through tube furnace under flowing air at 450 °C for 1 h with a heating ramp rate of 5 °C/min to yield sample designated as C-GaO. Part of sample C-GaO was further calcined under flowing air at 500 °C for 1 h with a heating ramp rate of 5 °C/min to yield sample MGaO. To generate GaN, a portion of the CMK-3/Ga composite was loaded into a gastight tube furnace and flushed with ammonia for 5 min. The sample was then heated at 5 °C/min to 900 °C and held for 4 h under the ammonia flow followed by cooling to room temperature under the ammonia flow to yield sample MGaN1.

Separately, GaN was also prepared as follows: 10 mL of a 1.0 M $GaCl_3$ toluene solution (the toluene solvent was a priori sodium dried) was added via dried syringe under stirring to 1.0 g of mesoporous carbon in a dry-sealed flask within a nitrogen

(13) (a) Zhao, D.; Yang, H. *J. Mater. Chem.* **2005**, *15*, 1217. (b) Roggenbuck, J.; Waitz, T.; Tiemann, M. *Microporous Mesoporous Mater.* **2008**, *113*, 575. (c) Liu, Q.; Wang, A.; Xu, J.; Zhang, Y. H.; Wang, X. D.; Zhang, T. *Microporous Mesoporous Mater.* **2008**, *116*, 461.
(14) Bois, L.; Dibandjo, P.; Chassagneux, F.; Sigala, C.; Miele, P. *J. Mater. Chem.* **2005**, *15*, 1917.
(15) Hou, Y.; Wang, X.; Wu, L.; Ding, Z. X.; Fu, X. Z. *Environ. Sci. Technol.* **2006**, *40*, 5799.
(16) (a) Kudo, A.; Mikami, I. *J. Chem. Soc., Faraday Trans.* **1998**, *94*, 2929. (b) Yanagida, T.; Sakata, Y.; Imamura, H. *Chem. Lett.* **2004**, *33*, 726.
(17) Arean, C. O.; Bellan, A. L.; Mentruit, M. P.; Delgado, M. R.; Palomino, G. T. *Microporous Mesoporous Mater.* **2000**, *40*, 35.
(18) Delgado, M. R.; Arean, C. O. *Mater. Lett.* **2003**, *57*, 2292.
(19) (a) Kam, K. C.; Deepak, F. L.; Gundiah, G.; Rao, C. N. R.; Cheetham, A. K. *Solid State Sci.* **2004**, *6*, 1107. (b) Chaplais, G.; Kaskel, S. *J. Mater. Chem.* **2004**, *14*, 1017. (c) Lin, C. N.; Huang, M. H. *J. Phys. Chem. C* **2009**, *113*, 925. (d) Fischer, A.; Muller, J. O.; Antonietti, M.; Thomas, A. *ACS Nano* **2008**, *2*, 2489. (e) Niederberger, M.; Garnweitner, G.; Pinna, N.; Neri, G. *Prog. Solid State Chem.* **2005**, *33*, 59.
(20) Zhao, D.; Feng, J.; Huo, Q.; Melosh, N.; Fredrickson, G. H.; Chmelka, B. F.; Stucky, G. D. *Science* **1998**, *279*, 548.
(21) Jun, S.; Joo, S. H.; Ryoo, R.; Kruk, M.; Jaroniec, M.; Liu, Z.; Ohsuna, T.; Terasaki, O. *J. Am. Chem. Soc.* **2000**, *122*, 10712.

filled glovebox. The resulting mixture was left for 1 h and then sonicated for 2 h, all under a flow of nitrogen. The sealed reaction flask was moved to a rotary evaporator (at ca. 30 °C) where a dry syringe was inserted through the seal, and the solvent was removed under a vacuum. A further 10 mL of 1.0 M $GaCl_3$ solution was added to the reaction flask followed by sonication and drying as described above under nitrogen. The resulting composite was further dried under an inert atmosphere in a sealed tube furnace at 150 °C for 2 h. The furnace was flushed with ammonia for 5 min and then heated at 5 °C/min to 1100 °C and held for 4 h under the ammonia flow followed by cooling to room temperature to yield sample MGaN2.

2.2. Material Characterization. Powder XRD analysis was performed using a Philips 1830 powder diffractometer with Cu Kα radiation (40 kV, 40 mA). Nitrogen sorption isotherms and textural properties of the materials were determined at −196 °C using nitrogen in a conventional volumetric technique by an ASAP 2020 sorptometer. Before analysis the samples were evacuated for 12 h at 40−200 °C under a vacuum. The surface area was calculated using the BET method based on adsorption data in the partial pressure (P/P_0) range 0.05 to 0.2 and total pore volume was determined from the amount of the nitrogen adsorbed at P/P_0 = ca. 0.99. Pore size distribution was determined using BJH analysis of adsorption data. Thermogravimetric analysis was performed using a Perkin-Elmer Pyris 6 TG analyzer with a heating rate of 5 °C/min in static air conditions. Transmission electron microscopy (TEM) images were recorded on a JEOL 2100F electron microscope operating at 200 kV. Samples examined by TEM were mounted on a support (holey carbon films on a copper mesh).

3. Results and discussion

3.1. Mesoporous Ga_2O_3. Mesoporous carbon CMK-3 was nanocasted using mesoporous silica SBA-15 as template. The mesoporous carbon was then used as hard template for nanocasting of mesostructured Ga_2O_3 using a toluene solution of $GaCl_3$ as precursor. The choice of precursor solvent was informed by the fact that hydrophobic mesoporous carbon is far more compatible with toluene solution (nonpolar toluene has a dielectric constant of 2.4 vs 80.1 for highly polar water). The XRD patterns of the silica and carbon templates are shown in Figure 1. The mesoporous silica exhibits three peaks, which we ascribe to the basal (100) diffraction (spacing of 80.3 Å), and (110) (200) diffractions from a hexagonal (*P6mm*) array of pores.[20] The CMK-3 carbon template exhibits one peak, which is the (100) diffraction of a hexagonal arrangement of pores with a basal spacing of 76.8 Å.[21] The low-angle region of the XRD pattern of the CMK-3/Ga composite shows a very weak shoulder; no clear peak is observed, which is consistent with filling of the carbon pores with the Ga precursor. Filling of the pores reduces the phase contrast between the carbon framework and pores, which reduces the intensity of the basal peak. The absence of a peak provides evidence of the successful pore filling of the gallium precursor into the pores of the carbon template. Such pore filling is essential for successful structural replication in the resulting gallium oxide.

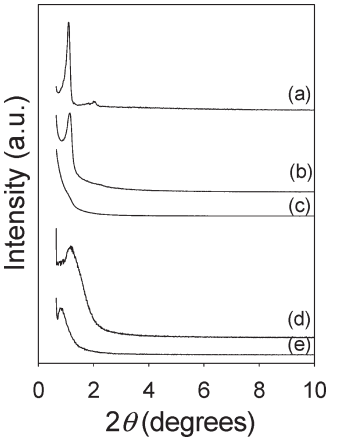

Figure 1. Powder XRD patterns of (a) SBA-15 silica, (b) CMK-3 carbon, (c) CMK-3/Ga composite, (d) C-GaO, and (e) MGaO.

Calcination/oxidation of the CMK-3/Ga composite in air was used to burn off the carbon and convert the gallium precursor into Ga_2O_3. We first point out that one calcination (at 500 °C), although successful in removing the carbon framework, generated disordered Ga_2O_3 products. To achieve replication of ordering in the gallium oxide, we adopted a two-step calcination strategy, first at 450 °C followed by 500 °C. The XRD pattern of sample C-GaO, which was obtained by calcination of the CMK-3/Ga composite at 450 °C for 1 h, exhibits a basal peak indicating retention of a mesostructured material. The basal spacing of the C-GaO sample (76.2 Å) is similar to that of the CMK-3 template. This suggests that sample C-GaO is dominated by the residual carbon framework, i.e., the basal peak arises from the carbon framework rather than any emerging Ga_2O_3 framework. However, the presence of a weak shoulder peak at lower 2θ values (Figure 1d) suggests the existence of an emerging framework distinct from the carbon. Indeed, following further calcination at 500 °C for 1 h, the resulting MGaO sample exhibits a basal peak at lower 2θ values with a spacing of 104 Å. For double templating, the basal spacing of MGaO should be similar to that of the SBA-15 and comparable to that of the CMK-3 template. The larger basal spacing of MGaO may be explained by a change in the pore geometry during the transformation of the carbon/Ga composites to mesoporous Ga_2O_3. Although it is clear that composite C-GaO has hexagonal ordering, it appears that on removal of the carbon, the generated MGaO sample adopts a lower level of mesostructural ordering with a wormhole type pore arrangement. The transformation from hexagonal to wormhole type pore arrangement may be driven by the fact that the formation of MGaO is not just an inverse replication from CMK-3 to Ga_2O_3, but an inverse replication that occurs along with a chemical change from $GaCl_3$ to Ga_2O_3, which may have implications on lattice size. Nevertheless, this is the first time that mesostructured Ga_2O_3 that exhibits a basal peak (an indication of fairly well ordered material) has been successfully prepared. The mode of carbon removal from the carbon/metal oxide composite appears to be a crucial step in the replication process.

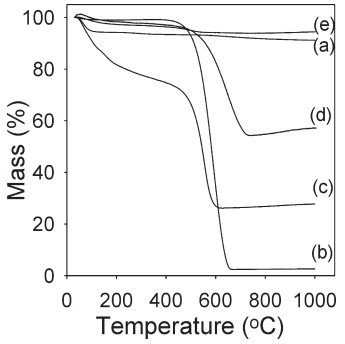

Figure 2. Thermogravimetric analysis curves of (a) SBA-15 silica, (b) CMK-3 carbon, (c) CMK-3/Ga composite, (d) C-GaO, and (e) MGaO.

Removal of the carbon framework is an important step in the formation of the mesoporous Ga_2O_3. It is necessary to confirm that no carbon is retained in the final Ga_2O_3 mesostructure and that the observed ordering arises from gallium oxide. Figure 2 shows thermogravimetric analysis (TGA) curves for the SBA-15 silica, CMK-3 carbon, and the CMK-3/Ga composite before and after calcination. The silica and carbon exhibit the expected weight loss trends with <3 wt % loss (due to removal of water) for the former and >98 wt % loss for the latter as the carbon is burned off. The TGA curve of the CMK-3/Ga composite indicates a weight loss of ca. 25 wt % at 400 °C that is due to removal of residual toluene, and weight loss of 49 wt % at 650 °C as the carbon framework is burnt off. The carbon content of the dry (toluene free) composite is therefore ca. 65 wt %, with the remainder (35 wt %) attributable to Ga_2O_3. Beyond 650 °C, after the carbon template has been removed, there is weight gain of ca. 1.5 wt % due to oxidation of residual gallium. A gallium oxide yield of 35 wt % in the composite (equivalent to 0.54 g Ga_2O_3 per g of carbon) is much higher than for previous carbon templated Ga_2O_3 solids,[22] and attests to the viability of the present route as a method for preparing mesostructured Ga_2O_3. The first calcination step at 450 °C (sample C-GaO) reduces the carbon content in the composite from 65 wt % to ca. 45 wt %. The TGA curve of sample MGaO shows no weight loss attributable to burning off of carbon, which confirms that the second calcination at 500 °C completely removes the carbon framework to generate Ga_2O_3. Elemental analysis confirmed the removal of carbon; only adventitious amounts of carbon were recorded. The formation of Ga_2O_3 is also confirmed by wide-angle XRD patterns (see Supporting Information, Figure 1S) that show the emergence of XRD peaks (at 2θ values of 35 and 63.5°) suggesting the existence of crystalline Ga_2O_3 domains in sample MGaO.[22]

The two-stage calcination of the carbon/Ga composite enables the formation of a mesoporous Ga_2O_3 framework. In the structural replication process, it is expected that the walls of the carbon framework (hard template) become the pore channels in the mesoporous Ga_2O_3. We have used transmission electron microscopy (TEM) to probe the replication process. TEM images reveal that the level of mesostructural ordering of the C-GaO composite is only slightly lower than that of the CMK-3 carbon template (see the Supporting Information, Figure 2S). For composite C-GaO to generate mesoporous Ga_2O_3 after further calcination, it must consist of two distinct frameworks; carbon and Ga_2O_3. In Figure 3, we compare two TEM images of sample C-GaO, one taken normally and the other taken using energy-filtered TEM (EFTEM) in which the carbon regions are bright. (In EFTEM, the electrons that interact with the sample are scattered inelastically and lose energy. The amount of energy lost is elementally sensitive. A magnetic prism and the use of slits directs electrons within a selected energy range to the detector). From the images, it is clear that there are two distinct frameworks, and more importantly, the EFTEM image shows evidence of a distinct Ga_2O_3 framework within the composite.

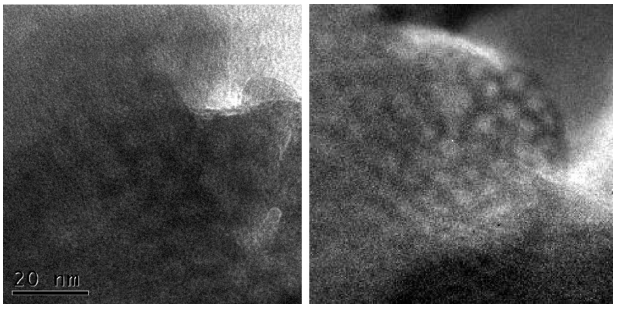

Figure 3. TEM (left) and EFTEM (right) image of C-GaO composite. The images are taken from the same region.

To further confirm the presence of a distinct Ga_2O_3 framework, we used electron energy loss spectroscopy (EELS) to map specific regions of the C-GaO composite. We note that unlike EFTEM, the EELS method collects electrons that pass directly through a thin piece of sample (i.e., through a region of sample not directly above either the Cu grid or holey carbon film support to ensure only the sample is analyzed). In practice, an electron beam is directed through the sample within a narrow range of kinetic energies. Inelastic scattering reduces the kinetic energy by amounts specific to particular elements. An electron spectrometer can then measure the quantity of electrons received that have had an inelastic interaction with an identifiable element through the slice of sample. The TEM image and zoomed region are shown along with the EELS spectra in Figure 4. The TEM micrograph shows the dark field image of the examined region, the zoomed image of where the spectra was taken (green box within top left image) and the spectra measured for the C K edge, Ga L edge, and O K edge energy detected is displayed in greyscale. It is clear that the C rich regions (CMK-3 framework) are distinct from the jointly Ga and O rich regions (Ga_2O_3 framework).

The TEM images for the mesoporous Ga_2O_3 product are shown in Figure 5. The images reveal a highly porous material with wormhole type pore channels, which is consistent with the XRD pattern in Figure 1. Mesoporous materials with wormhole type pores usually exhibit a

(22) Sun, X.; Li, Y. *Angew. Chem., Int. Ed.* **2004**, *43*, 3827.

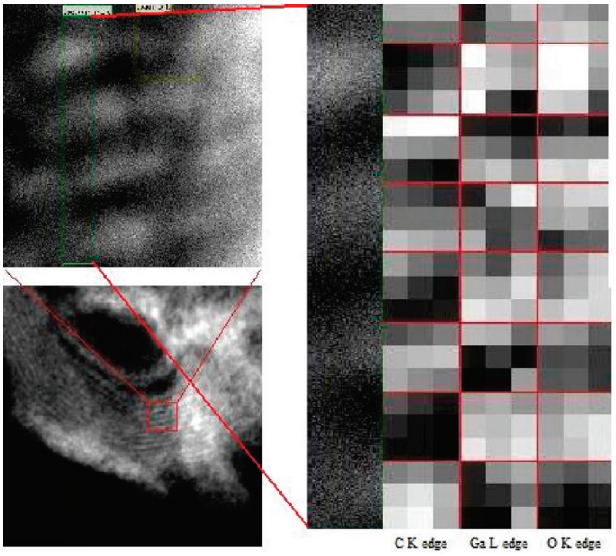

Figure 4. TEM image and EELS spectra of C-GaO composite. The EELS spectra were taken from the zoomed region of the TEM image (the green selection in the top left image shows the analyzed region).

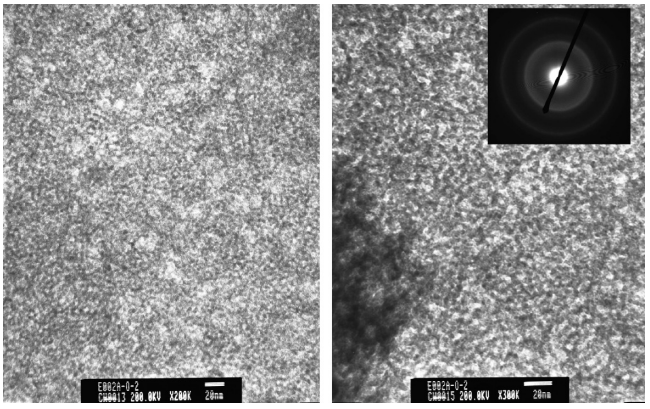

Figure 5. TEM images of mesoporous Ga_2O_3 (sample MGaO). The inset shows the corresponding selected area electron diffraction (SAED) pattern. The scale bar is 20 nm.

single basal peak.[4] The selected area electron diffraction (SAED) pattern (inset Figure 6) shows intense electron diffraction rings, consistent with partial crystallinity of the Ga_2O_3 walls (see the Supporting Information, Figure 1S). Higher-magnification TEM images (see the Supporting Information, Figure 3S) show further evidence of crystalline ordering within the walls of the mesoporous Ga_2O_3. The higher-magnification TEM images also show the wormhole type pore channels, and it is possible to estimate the wall thickness of the MGaO framework to be 55−60 Å.

The nitrogen sorption isotherm of the mesoporous Ga_2O_3 is shown in Figure 6. For comparison, we have included isotherms of the SBA-15 silica, carbon CMK-3 template and CMK-3/Ga composite before and after the first calcination at 450 °C (sample C-GaO). Figure 6 also shows the corresponding pore size distribution curves, and the textural properties are summarized in Table 1. The SBA-15 silica exhibits a type IV isotherm with a H1-type hysteresis loop, accompanied with high surface area

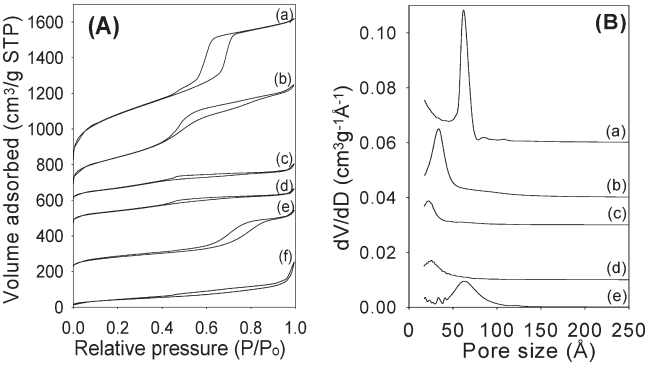

Figure 6. (A) Nitrogen sorption isotherms and (B) corresponding pore size distribution curves of (a) SBA-15 silica, (b) CMK-3 carbon, (c) CMK-3/Ga composite, (d) C-GaO, (e) MGaO, and (f) MGaN1. For clarity, the isotherms are offset (y-axis) as follows: (a) 700, (b) 600, (c) 600, (d) 400, (e) 200.

and pore volume, which is typical for a highly ordered mesoporous material.[23] The CMK-3 carbon also exhibits an isotherm typical of a well ordered mesoporous carbon with a well developed mesopore filling step, and the expected high surface area and pore volume.[24] The SBA-15 silica and carbon have sharp pore size distribution centered at 62 and 34 Å respectively. As expected, the isotherms of composites CMK-3/Ga and C-GaO show very little evidence of mesoporosity because of the infilling of the Ga precursor into the carbon pore system. The pore size distribution of composite CMK-3/Ga, with few pores centered at 22 Å indicates incomplete filling of the carbon pores. It is also possible that some porosity was created during evacuation at 40 °C under a vacuum (e.g., removal of residual toluene) prior to nitrogen sorption analysis. The average pore size slightly increases to 26 Å for sample C-GaO after the first calcination at 450 °C. On the other hand, sample MGaO exhibits a type IV isotherm with a H1-type hysteresis loop comparable to that of the SBA-15 silica. The isotherm indicates a significant level of mesotructural ordering, which is also evident from the relatively uniform pore size distribution with an average pore size of 63 Å. The pore size distribution of the mesoporous Ga_2O_3 (50−80 Å) is, however, rather broader than that of the SBA-15 silica. An average pore size of ca. 63 Å is consistent with the basal spacing of 104 Å (from XRD pattern in Figure 1e) and wall thickness of 55−60 Å (TEM images, see the Supporting Information, Figure 3S).

The surface area and pore volume of the SBA-15 and carbon are typical for such materials.[23,24] The surface area and pore volume of the CMK-3 carbon drastically reduced from 1181 m^2/g and 1.0 cm^3/g to 265 m^2/g and 0.32 cm^3/g (for composite CMK-3/Ga) after infilling of the Ga precursor. The textural properties slightly increase to 482 m^2/g and 0.41 cm^3/g after the first calcination at 450 °C because of removal of some carbon and dehydration of the Ga precursor. The final mesoporous Ga_2O_3 has surface area of 307 m^2/g and pore volume of 0.54 cm^3/g.

(23) Jaroniec, M.; Kruk, M. *Chem. Mater.* **2001**, *13*, 3169.
(24) (a) Lee, J.; Kim, J.; Hyeon, T. *Adv. Mater.* **2006**, *18*, 2073. (b) Liang, C.; Li, Z.; Dai, S. *Angew. Chem., Int. Ed.* **2008**, *47*, 3696.

Table 1. Textural Properties of Study Materials (see Experimental Section for Sample Description)

sample	basal spacing (Å)	surface area (m^2/g)	pore volume (cm^3/g)	pore size (Å)
SBA-15	80.2	1365	1.42	62
CMK-3	76.8	1181	1.00	34
CMK-3/Ga		265	0.32	22
C-GaO	76.2	482	0.41	26
MGaO	104.0	307	0.54	63
MGaN1		156	0.39	
MGaN2		136	0.33	

This is the highest surface area and pore volume ever reported for a mesoporous Ga_2O_3. The surface area is at least two times higher than any previous reports.[18,19] Furthermore, the present mesoporous Ga_2O_3 has the added advantage of being fairly well ordered according to the XRD, TEM, and porosity data. Recently, Ga_2O_3 has been shown to be an excellent photocatalyst with activity higher than that of benchmark TiO_2 catalysts.[25] The higher photocatalytic activity of Ga_2O_3 is explained by a higher band gap of 4.9 eV (for bulk Ga_2O_3) compared to 3.2 eV for TiO_2.[15,16,25] It is therefore important to confirm that the mesoporous MGaO sample has a similarly high band gap. We determined a band gap of 4.6 eV for the present mesoporous Ga_2O_3 (see the Supporting Information, Figure 4S). This band gap is similar to that of bulk gallium oxide materials, and in combination with surface area that is ca. 6 times higher should potentially result in enhanced photocatalytic activity for the mesoporous Ga_2O_3.

3.2. Mesoporous GaN. Nanoporous GaN (sample MGaN1) was synthesized via nitridation of the carbon/$GaCl_3$ composite at 900 °C. A highly crystalline form of GaN was generated as shown by XRD patterns (see the Supporting Information, Figure 5S). The XRD pattern of sample MGaN1 exhibits very sharp peaks characteristic of crystalline GaN and no other phases (e.g., Ga_2O_3) were present.[22] Thermal analysis of sample MGaN1 indicated no weight loss up to 1000 °C, which confirmed the absence of any carbonaceous impurities. Elemental analysis also indicated the absence of impurities. The nitrogen sorption isotherm of sample MGaN1 suggests the presence of significant porosity. However, the well ordered mesoporosity of MGaO is not clearly observed in MGaN1. TEM images (see the Supporting Information, Figure 6S) show that sample MGaN1 is made up of aggregated or loose nanoparticles/nanocrystals of size 50−80 nm. The porosity of MGaN1 is therefore largely due to interparticle voids. Nevertheless, sample MGaN1 exhibits a high surface area and pore volume of 156 m^2/g and 0.39 cm^3/g. These textural properties are much higher than those previously reported.[19] The size (50−80 nm) of the MGaN1 nanoparticles provides the basis for the high surface area observed.

We also prepared a second GaN sample (MGaN2) using greater amounts of $GaCl_3$ precursor via a sonication route followed by nitridation at a higher (1100 °C) temperature. The advantage of this route is that it reduced the amount of time required to impregnate the carbon template with Ga precursor and avoided any potential contact with air. A relatively crystalline MGaN2 sample (according to XRD pattern in the Supporting Information, Figure 5S) was generated. Thermal analysis (no mass loss on heating to 1000 °C) and elemental analysis (Ga and N element% > 96%) confirmed the absence of impurities. Sample MGaN2 had high surface area (136 m^2/g) and pore volume (0.33 cm^3/g). TEM images in Figure 7 show sample MGaN2 to have better porosity than MGaN2 but at a lower level of ordering compared to MGaO (Figure 5). The porosity of sample MGaN2 appears to be derived from templating (or confinement) effects that generate smaller stringy nanoparticles with a close packed arrangement that is permeated by pore channels. The size of the nanoparticles (5 −8 nm) is smaller than that of sample MGaN1. It is likely that for sample MGaN1, contact with air (during washing of the CMK-3/Ga composite) may cause growth of larger GaN nanoparticles during the subsequent nitridation step.

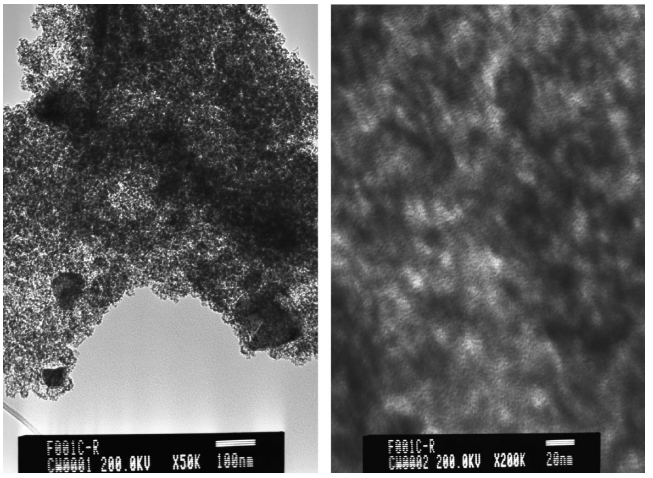

Figure 7. TEM images of mesoporous GaN (sample MGaN2).

4. Conclusions

In conclusion, we have shown that mesoporous Ga_2O_3 may be nanocast using mesoporous carbon as hard template via a carefully controlled replication route. We note that although this work involves double nanocasting, it can be simplified to one nanocasting step by using mesoporous carbons that are prepared directly via soft templating routes.[24] Infiltration of sufficient Ga molecular precursor (in the form of a toluene solution of $GaCl_3$) into the pores of the carbon template is essential and care must be taken to exclude contact with water during the nanocasting process. A two-stage calcination/oxidation

(25) Zhao, B.; Zhang, P. *Catal. Commun.* **2009**, *10*, 1184.

process, first at 450 °C and then at 500 °C, converts the $GaCl_3$ precursor within the carbon pore channels into a self-supporting Ga_2O_3 mesostructured framework that is retained after complete removal of the carbon. The resulting mesoporous Ga_2O_3 exhibits high surface area (307 m^2/g) and pore volume (0.54 cm^3/g), and bad gap energy of 4.6 eV. The textural properties are remarkable given that the mesostructured Ga_2O_3 contains significant crystallinity within the pore wall framework. Thermal treatment of the carbon/$GaCl_3$ composite in the presence of ammonia (nitridation) generates crystalline nanostructured GaN with a high surface area of 136−156 m^2/g and pore volume of 0.3−0.4 cm^3/g. Depending on the nanocasting route, the porosity of the GaN arises from voids between larger nanoparticles of size 50−80 nm or pore channels generated from a close-packed arrangement of templated smaller nanoparticles (5−8 nm). The high surface area mesoporous Ga_2O_3 and GaN materials may open up new opportunities in catalysis or high-temperature/high-power electronic devices where a large surface is essential.

Acknowledgment. We acknowledge the assistance of Dr. Mike Fay (Nottingham Nanotechnology and Nanoscience Centre) with the TEM analysis.

Supporting Information Available: Six additional figures: XRD patterns, TEM images, and diffuse reflectance absorption spectra of study materials (PDF). This material is available free of charge via the Internet at http://pubs.acs.org.